

# Traffic Density Control for Heterogeneous Highway Systems With Input Constraints

Arash Rahmanidehkordi<sup>®</sup> and Amir H. Ghasemi<sup>®</sup>, *Member, IEEE* 

Abstract—This letter introduces a traffic management algorithm for heterogeneous highway corridors consisting of both human-driven vehicles (HVs) and autonomous vehicles (AVs). The traffic flow dynamics are modeled using the heterogeneous METANET model, with variable speed control employed to maintain desired vehicle densities and reduce congestion. To generate speed control commands, we developed a hybrid framework that combines feedback linearization (FL) and model predictive control (MPC), treating the traffic system as an overactuated, constrained nonlinear system. The FL component linearizes the nonlinear dynamics, while the MPC component handles constraints by generating virtual control inputs that ensure control limits are respected. To address the over-actuated nature of the system, we introduce a novel constraint mapping algorithm within the MPC that links virtual control input constraints to the actual control commands. Additionally, we propose a real-time reference density generation method that accounts for both AVs and HVs to mitigate congestion. Numerical simulations were conducted for two scenarios: controlling only AVs and controlling both AVs and HVs. The results demonstrate that the proposed FL-MPC framework effectively reduces congestion, even when speed control is applied exclusively to AVs.

Index Terms—Traffic control, feedback linearization, heterogeneous systems, model predictive control.

## I. INTRODUCTION

RAFFIC control on heterogeneous traffic highways, with both AVs and HVs, presents unique challenges [1]. While AV integration can improve traffic flow, reduce congestion, and enhance safety, effective control strategies must address nonlinearity, uncertainty, and regulatory state and control input constraints. Among traffic control methods for large-scale highways, feedback control-based approaches are often preferred for their simplicity and robustness, especially compared to the more computationally demanding MPC-based techniques [2], [3]. In highway traffic control,

Received 16 September 2024; revised 12 November 2024; accepted 29 November 2024. Date of publication 11 December 2024; date of current version 18 December 2024. This work was supported by the National Science Foundation under Grant 2130704. Recommended by Senior Editor C. Manzie. (Corresponding author: Arash Rahmanidehkordi.)

The authors are with the Department of Mechanical Engineering, University of North Carolina at Charlotte, Charlotte, NC 28262 USA (e-mail: arahmani@charlotte.edu; ah.ghasemi@charlotte.edu).

Digital Object Identifier 10.1109/LCSYS.2024.3516073

maintaining the desired density is crucial for preventing congestion [4]. Variable speed control is an effective approach for achieving this. FL is particularly promising for determining speed commands, as it simplifies the complex nonlinear dynamics of heterogeneous traffic systems. However, speed constraints, bounded between zero and the maximum limit, pose challenges for traditional FL methods, often resulting in suboptimal or infeasible solutions [3]. To address this limitation, feedback linearization can be combined with an MPC algorithm to form an FL-MPC hybrid controller [5], [6]. In this approach, the virtual control input of FL is determined via MPC to ensure the actual control commands stay within the required bounds. However, since traffic velocities are constrained to be non-negative, applying the FL-MPC method from [5], [6] may lead to infeasibility. This is because achieving full controllability within these constraints requires treating the traffic control problem as an over-actuated system, and using the Moore-Penrose pseudoinverse for constraint mapping, as in [5], [7], does not always guarantee a solution for the virtual control command.

To overcome the limitations of the FL-MPC approach, we introduced a novel constraint mapping algorithm that links the bounds of the actual control inputs to the virtual control inputs of FL. By utilizing the null space of the control input matrix, the algorithm generates multiple candidate matrices that ensure system constraints are met. The optimal matrix is then chosen by solving an MPC problem that minimizes the cost function, thereby guaranteeing feasible control inputs and effectively balancing desired traffic density with control limits [8]. Building on the core control algorithm from our previous work [8], this letter significantly advances its application by adapting it to a more complex system, a heterogeneous traffic model, instead of the previously addressed homogeneous network.

In addition to handling input constraints, determining the reference commands is another crucial challenge in designing feedback controllers, including FL for heterogeneous traffic highways. Unlike homogeneous traffic, which uses critical density as a reference, a more intricate approach is required for heterogeneous highways. To our knowledge, no existing work has yet addressed the selection of reference commands in heterogeneous traffic networks. This study proposes a method to determine and update the density reference commands in real-time consider each cell's congestion proximity and the AV-to-HV ratio, ensuring neither vehicle class is overly

2475-1456 © 2024 IEEE. All rights reserved, including rights for text and data mining, and training of artificial intelligence and similar technologies. Personal use is permitted, but republication/redistribution requires IEEE permission. See https://www.ieee.org/publications/rights/index.html for more information.

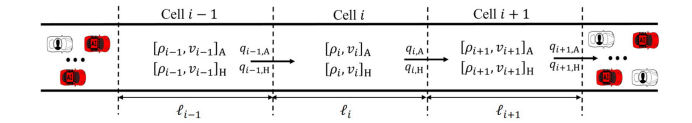


Fig. 1. Schematic of a traffic network divided into cells, showing state variables: density  $(\rho_{i,A}, \rho_{i,H})$ , velocity  $(v_{i,A}, v_{i,H})$ , and outflow  $(q_{i,A}, q_{i,H})$  for AVs and HVs.

restricted in movement. The simulation results demonstrate that integrating the proposed density reference generation approach with the FL-MPC controller effectively reduces congestion in heterogeneous traffic highways, even when control commands are provided only to AVs and not necessarily to HVs.

This letter is structured as follows: Section II introduces the METANET model for macroscopic flow dynamics in heterogeneous traffic. Section III discusses maintaining desired traffic densities with the FL-MPC approach and mapping control constraints. Section IV presents simulation results showing the effectiveness of FL-MPC in reducing congestion with control applied only to AVs. Section V concludes with future research directions.

# II. MACROSCOPIC FLOW DYNAMICS OF HETEROGENEOUS TRAFFIC ON HIGHWAY CORRIDOR

Consider a heterogeneous highway corridor including AVs and HVs. To model and analyze the traffic flow within these corridors, we utilize the heterogeneous METANET model described in [9]. For this purpose, the highway is discretized into n cells, denoted as  $\mathcal{C}_i$ , each characterized by a length  $\ell_i$  and the number of lanes  $\gamma_i$ , where  $i \in \{1, 2, ..., n\}$ . The populations of AVs and HVs in each cell are represented as  $n_{i,A}$  and  $n_{i,H}$ , respectively, as depicted in Fig. 1.

Let us define the state vector for the entire traffic system along the corridor as  $x = [x_1, x_2, ..., x_n]^T$ , where  $x_i = [\rho_{i,A}, \rho_{i,H}, v_{i,A}, v_{i,H}]^T$ . Here,  $\rho_{i,c} = n_{i,c}/\ell_i$  and  $v_{i,c}$  represent the density and average velocity of vehicles in class c, with  $c \in \{AVs, HVs\}$ . The changes in the densities within cell  $\mathcal{C}_i$  follow the law of conservation of vehicles and can be expressed as

$$\dot{\rho}_{i,c}(t) = \frac{1}{\ell_i \gamma_i} \Big( q_{i-1,c}(t) - q_{i,c}(t) \Big), \tag{1}$$

where  $q_{i,c} = \rho_{i,c} v_{i,c}$  represents the outflows of vehicle class c from cell  $C_i$ .

In the heterogeneous METANET model, the evolution of velocities  $v_{i,c}$ , along with the interaction between vehicle classes, is predicated on the assumption that a triangular fundamental diagram can depict their macroscopic behavior in homogeneous scenarios (see Fig. 2). Parameters like capacity flows  $C_c$ , critical densities  $\rho_{\text{critm,c}}$ , free-flow speeds  $v_{\text{ff,c}}$ , and maximum densities  $\rho_{\text{Jam,c}}$  are defined for each vehicle class, with AVs assumed to have higher values for these in this research [see Fig. 2(a)].

The velocity changes within the heterogeneous METANET model can be derived by

$$\dot{v}_{i,c}(t) = \frac{1}{\tau_c} \left( U_{i,c} - v_{ic} \right) + \frac{1}{\ell_i} v_{i,c} \left( v_{i-1,c} - v_{i,c} \right) - \frac{\eta_c}{\ell_i \tau_c} \left( \frac{\rho_{i+1,c} - \rho_{i,c}}{\rho_{i,c} + \kappa_c} \right), \tag{2}$$

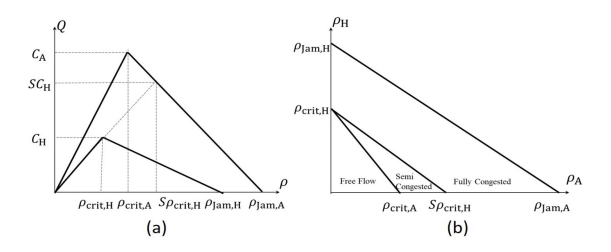


Fig. 2. (a) Fundamental diagrams for two vehicle classes: AVs and HVs. (b) Three traffic regimes in a mixed traffic system: free flow, semi-congested, and fully congested.

where  $\tau_c$ ,  $\eta_c$ , and  $\kappa_c$  are class-dependent parameters. Specifically,  $\tau_c$  represents the aggregated traffic response to changes in density,  $\eta_c$  reflects the sensitivity to changes in the downstream density, and  $\kappa_c$  ensures the applicability of the model at high densities while preventing oversensitivity at low densities. Furthermore,  $U_{i,c}$  is the suggested velocity for each vehicle class, which serves as the control command to the traffic system. In the present work, we define  $U_{i,c}$  as a composition of two parts as expressed as follows:

$$U_{i,c} = (1 - u_{i,c})V_{i,c},\tag{3}$$

where  $0 \le u_{i,c} \le 1$  represents the regulatory control input, and  $V_{i,c}$  refers to the desired or target speeds that each vehicle class aims to maintain in the absence of active traffic control interventions, such as variable speed limits. Here, we define  $V_{i,c}$  as [9],

$$V_{i,c}(t) = v_{\text{ff,c}} e^{\left[\frac{-1}{a_c} \left(\frac{\rho_{i,c}(t)}{\rho_{\text{crit},c}(t)a_{i,c}(t)}\right)^{a_c}\right]},\tag{4}$$

where  $a_c$  is a density-dependent parameter and  $\alpha_{i,c}$  is the class-dependent dynamic coupling terms that characterize the interaction between AVs and HVs and are influenced by their ratio and the total number of vehicles within cell  $\mathcal{C}_i$ .

Several methods exist to define  $\alpha_{i,c}$  [10]. In this letter, we use the user-equilibrium model for its accuracy in capturing AVs-HVs interactions at a macroscopic level. Assuming AVs have higher free-flow speeds and both vehicle classes share the highway, we define three traffic phases:

- Free-Flow Phase: AV and HV travel at their respective free-flow speeds  $(v_{\rm ff,\,H} \approx V_{i,\rm H} < V_{i,\rm A} \approx v_{\rm ff,\,A})$ . The coupling terms are determined as  $\alpha_{i,\rm H} = \rho_{i,\rm H}/(\rho_{\rm crit,\,H}(\frac{\rho_{i,\rm H}}{\rho_{\rm crit,\,H}} + \frac{\rho_{i,\rm A}}{\rho_{\rm crit,\,A}}))$  and  $\alpha_{i,\rm A} = 1 \alpha_{i,\rm H}$ .
   Semi-Congested Phase: HVs travel at their free flow
- Semi-Congested Phase: HVs travel at their free flow speed while the AVs enter congestion. Here, AVs travel at a speed less than their free-flow speed but more than the free-flow speed of HVs ( $v_{\rm ff,\,H} \approx V_{i,\rm H} \leq V_{i,\rm A} < v_{\rm ff,\,A}$ ). The coupling terms are calculated as  $\alpha_{i,\rm H} = \rho_{i,\rm H}/\rho_{\rm crit,\,H}$ , and  $\alpha_{i,\rm A} = 1 \alpha_{i,\rm H}$ .
- Congested Phase: AVs and HVs are congested and travel with the same velocity, which is less than the HVs' free-flow velocity ( $V_{i,H} = V_{i,A} < v_{ff,H} < v_{ff,A}$ ). The coupling terms are obtained by solving  $V_{i,A}(\rho_{i,A}/\alpha_{i,A}) = V_{i,H}(\rho_{i,H}/\alpha_{i,H})$  and  $\alpha_{i,H} + \alpha_{i,A} = 1$ .

Once, the dynamics coupling terms are determined, the total steady-state flow in cell  $C_i$  can be determined as:

$$Q_{i} = \rho_{i,A} V_{i,A} \left( \frac{\rho_{i,A}}{\alpha_{i,A}} \right) + \rho_{i,H} V_{i,H} \left( \frac{\rho_{i,H}}{\alpha_{i,H}} \right).$$
 (5)

the three traffic flow models and dynamic coupling terms assume steady-state conditions, where traffic is in equilibrium [10], [11]. However, in this letter, the system may be in a transient state when determining  $\alpha_c$ . Despite this, we compute the dynamic coupling terms based on a snapshot, assuming steady-state at that moment.

# III. MAINTAINING DESIRED TRAFFIC DENSITY WITH FL-MPC CONTROL

In highway traffic control, maintaining the desired density is essential for preventing congestion. This section outlines the design of a variable speed control algorithm that integrates FL with MPC to ensure speed commands remain within practical limits while achieving the desired density.

#### A. Feedback Linearization

For cell  $\mathcal{C}_i$ , let us define the desired reference density for AVs and HVs as  $\rho_{i,c}^* = [\rho_{i,A}^* \ \rho_{i,H}^*]^T$ . The FL controller seeks to determine the recommended velocities  $U_{i,c}$  for each vehicle class to minimize the error  $e_{i,c} = \rho_{i,c}^* - \rho_{i,c}$ . In this approach, we differentiate the output (density, in this case) up to the point where the input term appears [12]. Assuming density as the measurable output, i.e.,  $y_{i,c} = \rho_{i,c}$ , the input term appears at second derivative as

$$\ddot{y}_{i,c} = \ddot{\rho}_{i,c} = f_{i,c} + \left[ g_{i,c} \ \bar{g}_{i,c} \right] \begin{bmatrix} u_{i,c} \\ u_{i-1,c} \end{bmatrix}, \tag{6}$$

where

$$f_{i,c} = \frac{1}{\ell_{i}\gamma_{i}} \left( \dot{\rho}_{i-1,c} v_{i-1,c} - \dot{\rho}_{i,c} v_{i,c} + \psi_{i-1,c} - \psi_{i,c} \right),$$

$$\psi_{i,c} = \left( \frac{\rho_{i,c}}{\ell_{i}} \left( v_{i,c} (v_{i-1,c} - v_{i,c}) - \frac{\eta_{c}}{\tau_{c}} \frac{\rho_{i+1,c} - \rho_{i,c}}{\rho_{i,c} + \kappa_{c}} \right) - \frac{\rho_{i,c}}{\tau_{c}} v_{i,c} + \frac{\rho_{i,c} V_{i,c}}{\tau_{c}} \right),$$

$$g_{i,c} = \frac{\rho_{i,c} V_{i,c}}{\ell_{i}\gamma_{i}\tau_{c}} \qquad \bar{g}_{i,c} = -\frac{\rho_{i-1,c} V_{i-1,c}}{\ell_{i}\gamma_{i}\tau_{c}}$$

As shown in (6),  $\ddot{y}_{i,c}$  depends on both upstream inflow and downstream outflow. To ensure the flow remains non-negative and within the limits of the fundamental diagram, controlling the density in cell  $\mathcal{C}_i$  requires at least two control inputs, such as  $u_{i-1,c}$  and  $u_{i,c}$ , for the highway system to be fully controllable. By adjusting these inputs, reducing the upstream velocity decreases the inflow and density in  $\mathcal{C}_i$ , while reducing the velocity in  $\mathcal{C}_i$  increases its density. Expanding (6) to m adjacent cells, from  $\mathcal{C}_{i-m+1}$  to  $\mathcal{C}_i$ , gives

$$\ddot{\rho}_c = F_c + G_c u_c,\tag{7}$$

where  $u_c = [u_{i,c}, u_{i-1,c}, \dots, u_{i-m,c}]^T \in \mathbb{R}^{m+1}, F_c = [f_{i,c}, f_{i-1,c}, \dots, f_{i-m+1,c}]^T \in \mathbb{R}^m$ , and

$$G_{c} = \begin{bmatrix} g_{i,c} & \bar{g}_{i,c} & 0 & \cdots & 0 \\ 0 & g_{i-1,c} & \bar{g}_{i-1,c} & \cdots & 0 \\ \vdots & \vdots & \vdots & \ddots & \vdots \\ 0 & \cdots & 0 & g_{i-m+1,c} & \bar{g}_{i-m+1,c} \end{bmatrix}.$$

Let us define  $H_c \in \mathbb{R}^{(m+1)\times m}$  such that

$$G_C \times H_C = I_m \in \mathbb{R}^{m \times m}$$
. (8)

Then, the FL control command is derived as

$$u_c = H_c \left[ -F_c + \nu_c \right]. \tag{9}$$

Substituting (9) in (7), the output dynamics of FL is:

$$\ddot{\rho}_c = \nu_c. \tag{10}$$

Let  $\rho_c = [\rho_{i,c}, \dots, \rho_{i-m+1,c}]^{\mathrm{T}}$  be the density vector and  $\nu_c = [\nu_{i,c}, \dots, \nu_{i-m+1,c}]^{\mathrm{T}} \in \mathbb{R}^m$  the virtual control input vector. Typically,  $\nu_c$  is given as  $\nu_c = \ddot{\rho}_c^* + \beta_1(\dot{\rho}_c^* - \dot{\rho}_c) + \beta_0(\rho_c^* - \rho_c)$ , with constants  $\beta_1$  and  $\beta_0$  chosen to ensure Hurwitz dynamics. However, in highway traffic control,  $\nu_c$  must ensure  $u_c$  remains within bounds  $0 \le u_c \le u_{c,\max} \le 1$ , where  $u_{c,\max} = [u_{i,c,\max}, \dots, u_{i-m,c,\max}]^{\mathrm{T}}$ . Here,  $u_c = 0$  represents no command being applied, while  $u_c = 1$  indicates a full braking command for the vehicles. To address this, we determine  $\nu_c$  using an MPC approach.

#### B. Virtual Command Determination via MPC

This section presents the design of an MPC for computing the virtual control input vector  $v_c$  for the FL controller. Let us define the state vector  $\xi_c \in \mathbb{R}^{2m}$  as  $\xi_c = [\rho_c \ \dot{\rho}_c]^T$ . The discrete-time state-space representation of the output dynamics of the FL controller, from (10), are given by

$$\xi_c(k+1) = \bar{A}_{MPC} \, \xi_c(k) + \bar{B}_{MPC} \, \nu_c(k),$$
 (11a)

$$y_c(k) = \bar{C}_{MPC} \, \xi_c(k), \tag{11b}$$

where  $\bar{A}_{MPC}$ ,  $\bar{B}_{MPC}$ , and  $\bar{C}_{MPC}$  are discrete-time versions of the following matrices, using zero-order hold (ZOH):

$$A_{\text{MPC}} = \begin{bmatrix} 0_m & I_m \\ 0_m & 0_m \end{bmatrix}, \ B_{\text{MPC}} = \begin{bmatrix} 0_m \\ I_m \end{bmatrix},$$

$$C_{\text{MPC}} = [I_m \, 0_m]. \tag{12}$$

The virtual control input vector  $v_c$  is obtained by solving the following MPC optimization problem:

$$\min_{V_c(k)} J_c = \sum_{j=0}^{N_p} \left( \| y_c(k+j) - \rho_c^*(k+j) \|_{\Omega}^2 + \| \nu_c(k+j) \|_R^2 + \| \Delta \nu_c(k+j) \|_{S}^2 \right) \tag{13}$$

subject to the dynamics outlined in (11) and  $v_{c,\min} \leq v_c \leq v_{c,\max}$  where  $v_{c,\min}$  and  $v_{c,\max}$  are bounds on  $v_c$ . In (13),  $\mathbb{Q}$ , R, and S represent the weight matrices,  $N_p$  is the prediction horizon, and  $V_c(k) = [v_c(k|k), \ldots, v_c(k+N_u|k)]^T$  denotes the decision vector, where  $N_u$  is the control horizon. The weight matrix  $\mathbb{Q}$  tracks reference densities, R limits excessive commands (avoiding unnecessary braking), and S ensures smooth transitions in  $v_c$ . Also,  $\rho_c^* = [\rho_{i,c}^*, \ldots, \rho_{i-m+1,c}^*]^T$  is the reference signal. The decision vector  $v_c$  must satisfy the condition  $0 \leq u_c \leq u_{c,\max}$ . Accordingly, a constraint mapping algorithm is needed to link the bounds on  $u_c$  to the bounds on  $v_c$ 

#### C. Constraint Mapping Algorithm

To establish the relationship between the bounds of  $u_c$  and  $v_c$ , the control law in (9) can be reformulated as

$$H_c v_c = H_c F_c + u_c, \tag{14}$$

considering the bounds over  $u_c$  yields

$$H_c F_c \le H_c \nu_c \le H_c F_c + u_{c.\text{max}}. \tag{15}$$

Both  $F_c$  and  $G_c$  are state-dependent and vary over time, requiring  $H_c$  to be computed in real time. Since  $H_c$  is an  $m+1 \times m$  matrix, there are m+1 inequalities but only m unknowns for  $\nu_c$ , making the system overdetermined. Although there are infinite choices for  $H_c$  that satisfy (8), the Moore-Penrose pseudoinverse is commonly used, i.e.,  $H_c = G_c^{\dagger}$ . However, choosing  $H_c = G_c^{\dagger}$  does not always guarantee a feasible solution for  $\nu_c$  under (15). For instance, if the control block is a single cell  $\mathcal{C}_i$ , the Moore-Penrose pseudoinverse would be:

$$H_{c} = G_{c}^{\dagger} = G_{c}^{T} (G_{c} G_{c}^{T})^{-1}$$

$$= \begin{bmatrix} g_{i,c} \\ \bar{g}_{i,c} \end{bmatrix} ( [g_{i,c} \quad \bar{g}_{i,c}] \begin{bmatrix} g_{i,c} \\ \bar{g}_{i,c} \end{bmatrix} )^{-1} = \begin{bmatrix} \frac{g_{i,c}}{g_{i,c}^{2} + \bar{g}_{i,c}^{2}} \\ \frac{g_{i,c}}{g_{i,c}^{2} + \bar{g}_{i,c}^{2}} \end{bmatrix}, (16)$$

considering (15) the constraints on  $v_c$  can be expressed as

$$\frac{g_{i,c}f_{i,c}}{g_{i,c}^2 + \bar{g}_{i,c}^2} \le \frac{g_{i,c} v_c}{g_{i,c}^2 + \bar{g}_{i,c}^2} \le \frac{g_{i,c}f_{i,c}}{g_{i,c}^2 + \bar{g}_{i,c}^2} + u_{i,c,\max}, \quad (17a)$$

$$\frac{\bar{g}_{i,c}f_{i,c}}{g_{i,c}^2 + \bar{g}_{i,c}^2} \le \frac{\bar{g}_{i,c} v_c}{g_{i,c}^2 + \bar{g}_{i,c}^2} \le \frac{\bar{g}_{i,c}f_{i,c}}{g_{i,c}^2 + \bar{g}_{i,c}^2} + u_{i,c,\text{max}}. \quad (17b)$$

Dividing (17a) and (17b) by  $\frac{g_{i,c}}{g_{i,c}^2 + \bar{g}_{i,c}^2} > 0$  and  $\frac{\bar{g}_{i,c}}{g_{i,c}^2 + \bar{g}_{i,c}^2} < 0$ , respectively, yields

$$f_{i,c} \le \nu_c \le f_{i,c} + \frac{g_{i,c}^2 + \bar{g}_{i,c}^2}{g_{i,c}} u_{i,c,\max},$$
 (18a)

$$f_{i,c} \ge \nu_c \ge f_{i,c} + \frac{g_{i,c}^2 + \bar{g}_{i,c}^2}{\bar{g}_{i,c}} u_{i,c,\text{max}}.$$
 (18b)

From (18), it becomes evident that when  $H_c = G_c^{\dagger}$ , the two inequalities intersect at the single point  $v_c = f_{i,c}$ , making this the only feasible selection for  $v_c$ . Taking this into account for a single cell  $C_i$ , where  $F_c = f_{i,c}$ , substituting the single point answer of  $v_c$  in (14), results in  $u_c = 0$ . In other words, it may be interpreted as we always apply the same command  $u_c = 0$  to our system. This means that the suggested velocity  $U_{i,c}$  for each vehicle class is the same as speed without any active interventions  $V_{i,c}$  (see (3)). Therefore, selecting  $H_c = G_c^{\dagger}$  is not a feasible solution for a highway traffic control system.

The crux of this letter is to address this issue by introducing a new constraint mapping algorithm, selecting  $H_c$  to satisfy (8) and ensure a solution interval for  $v_c$  in (15). We propose an algorithm that generates a set of candidate  $H_c$  matrices, each of which satisfies the constraint in (15). Since  $G_c$  is a non-square matrix with more columns than rows, it consistently has full row rank m. As a result,  $G_c$  has a null space of dimension 1, i.e.,  $\dim(\mathcal{N}(G_c)) = 1$ . Let  $\varphi_c$  be a basis for the one-dimensional vector space  $(\varphi_c \subset \mathcal{N}(G_c)) \in \mathbb{R}^{m+1}$ . Since the Moore-Penrose pseudoinverse matrix  $G_c^{\dagger}$  satisfies (8), then adding any linear combination of the vector  $\varphi_c$  to its columns will still satisfy (8). In particular,  $G_c$  ( $G_c^{\dagger} + \Phi_c \Lambda_c$ ) =  $I_m$ , where  $\Phi_c = [\varphi_c, \dots, \varphi_c] \in \mathbb{R}^{(m+1) \times m}$  is a matrix whose columns are the null space basis and  $\Lambda_c = \operatorname{diag}([\lambda_1, \dots, \lambda_m]) \in \mathbb{R}^{m \times m}$  which its elements  $\lambda_1, \dots, \lambda_m$  can

be arbitrary numbers. Therefore, the matrix  $H_c$  can be defined as

$$H_c = G_c^{\dagger} + \Phi_c \Lambda_c. \tag{19}$$

To guarantee that (15) has a solution, we must reduce the system of m+1 to m inequalities. This can be achieved by selecting  $\Lambda^{\hat{i}} = \text{diag}([\lambda^{\hat{i}}_1, \dots, \lambda^{\hat{i}}_m])$ , ensuring that the  $\hat{i}$ -th row of  $H_c$  becomes zero. The resulting matrix  $H_c$  with its  $\hat{i}$ -th row being zero is then can be expressed as

$$H_{\hat{i},c} = G_c^{\dagger} + \Phi_c \Lambda_c^{\hat{i}} = \begin{bmatrix} h_{11}^{\hat{i},c} & \dots & h_{1m}^{\hat{i},c} \\ \vdots & & \vdots \\ h_{(\hat{i}-1)1}^{\hat{i},c} & \dots & h_{(\hat{i}-1)m}^{\hat{i},c} \\ 0 & \dots & 0 \\ h_{(\hat{i}+1)1}^{\hat{i},c} & \dots & h_{(\hat{i}+1)m}^{\hat{i},c} \end{bmatrix} \leftarrow \hat{i}^{\text{th}}. (20)$$

$$\vdots & & \vdots \\ h_{(m+1)1}^{\hat{i},c} & \dots & h_{(m+1)m}^{\hat{i},c} \end{bmatrix}$$

By selecting the elements of  $\Lambda_c^{\hat{i}}$  and applying  $H_{\hat{i},c}$  to the inequality in (15), the constraint for the  $\hat{i}$ -th row simplifies to the trivial condition  $0 \le 0 \le u_{c,\max}$ . Next, let  $\hat{H}_{\hat{i},c}$  denotes the resulting square matrix of size  $m \times m$ , obtained by eliminating the zero row from  $H_{\hat{i},c}$ . The inequality (15) can be rewritten in the solvable form as

$$\hat{H}_{\hat{i},c} F_c \le \hat{H}_{\hat{i},c} \nu_c \le \hat{H}_{\hat{i},c} F_c + u_{c,\text{max}}.$$
 (21)

Since  $H_c$  has m+1 rows, there are m+1 possible  $\Lambda^{\hat{i}}$  matrices that can zero a row of  $H_c$  for  $1 \leq \hat{i} \leq m+1$ . Consequently, there are m+1 candidate square, full-rank, invertible matrices  $\hat{H}_{\hat{i},c} \in \{\hat{H}_{1,c}, \hat{H}_{2,c}, \dots, \hat{H}_{m+1,c}\}$ . To select the best matrix, the MPC problem is solved for each candidate and the optimal matrix  $\hat{H}_c^*$ , which resulted in a minimum cost  $J_c^*$ , is chosen. The virtual control input vector  $\nu_c^*$  calculated for the MPC problem with cost value  $J_c^*$  is then applied into FL control command  $u_c^*$  as expressed in (9).

# D. Reference Density Signal Generation in Heterogeneous Traffic Systems

To determine the virtual control command  $v_c$ , the objective function in (13) requires knowledge of the reference signal  $\rho_{i,c}^*$ . In a congested homogeneous traffic system, the critical density  $\rho_{\text{crit},c}$  where the maximum flow occurs [see Fig. 3(a)] can be used as the desired density of the cell. However, in a heterogeneous traffic network, this problem becomes more complex. As described in Section II, for a two-class highway traffic system, three distinct traffic flow phases can be identified. These phases, represented as functions of AVs and HVs densities, are illustrated in Fig. 2(b).

For a cell in the congested phase [indicated by the green cross in Fig. 3(b)], the traffic management goal is to guide the system towards free-flow conditions. Fig. 3(a) illustrates the total steady flow Q as a function of AVs and HVs densities. It is evident that focusing solely on flow maximization, without considering the vehicle classes, could result in halting all

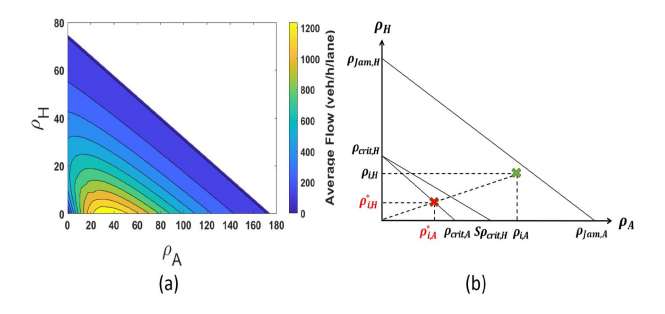


Fig. 3. (a) Total steady-state flow contour and (b) Reference density signal generation for cell  $\mathcal{C}_i$ .

## Algorithm 1 FL-MPC Algorithm

- 1: Measure current states and determine the reference commands  $\rho_c^*$ . Update matrices  $G_c$  and  $F_c$  based on new states as described in Section III-A.
- 2: Find  $\varphi_c$ , the single basis of the null space  $\mathcal{N}(G_c)$
- 3: Determine  $\Lambda^{\hat{i}}$  such that i<sup>th</sup> row of  $H_c$  becomes zero.
- 4: Generate the set  $\hat{H}_{\hat{i},c} \in \{\hat{H}_1, \hat{H}_2, \dots, \hat{H}_{m+1}\}$  by removing the zero  $\hat{i}$ th row from  $H_c$ .
- 5: Solve the MPC optimal control problem (13) m+1 times for all sets  $\hat{H}_{\hat{i},c}$ , subject to (21).
- 6: Select the MPC decision vector  $v_c^*$  with the least cost among the cases  $J_c^*$  and determine  $u_c^*$  based on (9).
- 7: Apply  $u_c^*$  to the system and return to Step 1.

HVs, which is not a feasible solution. A more balanced approach is needed to determine the optimal density without disadvantaging either vehicle class.

To set the desired densities for each cell, the values  $\rho_{i,A}^*$  and  $\rho_{i,H}^*$  are determined by drawing a line from the cell's current density position  $(\rho_{i,A}, \rho_{i,H})$  to the origin. The point where this line intersects the boundary of the free-flow region, indicated by the red cross in Fig. 3(b), is set as the desired density. Defining the desired density vector this way allows the reference point to adjust dynamically based on congestion proximity and the AVs to HVs ratio within the cell. This approach prevents full restriction of either class, maintaining optimal flow and space for both.

In summary, the hybrid FL-MPC controller, designed for nonlinear-constrained-over-actuated heterogeneous traffic highway, can be outlined in the following algorithm.

## IV. RESULTS AND DISCUSSION

This section evaluates the effectiveness of the proposed reference generation algorithm combined with FL-MPC in reducing congestion in a heterogeneous traffic network using variable speed control. For this study, we consider a 3-lane highway corridor divided into 8 cells, each with a length of 2 km ( $\ell_i = 2$ , km). The METANET model parameters for each vehicle class are provided in Table I [11], [13].

We initialize the densities of cells 1 to 8 as follows:  $\rho_A = [7, 11, 14, 49, 19, 49, 17, 14]^T$  and  $\rho_H = [4, 6, 8, 26, 11, 26, 10, 8]^T$  (veh/km/lane). With these initial densities, cells  $\mathcal{C}_4$ ,  $\mathcal{C}_5$ , and  $\mathcal{C}_6$  are in congestion, with  $\mathcal{C}_4$  and  $\mathcal{C}_6$  approaching jam conditions (i.e., near the line connecting

TABLE I
HETEROGENEOUS METANET MODEL PARAMETERS

Parameter	Unit	AVs	HVs
$ ho_{ m crit,c}$	veh/km/lane	34.7349	18.9261
$ ho_{ m J,c}$	veh/km/lane	175	75
$v_{ m ff,c}$	km/h	106.34	82.80
$a_{ m c}$	_	1.6761	2.1774
$ au_{ m c}$	S	18	18
$\kappa_{ m c}$	veh/km/lane	40	40
$\eta_{ m c}$	$\mathrm{km^2/h}$	60	60

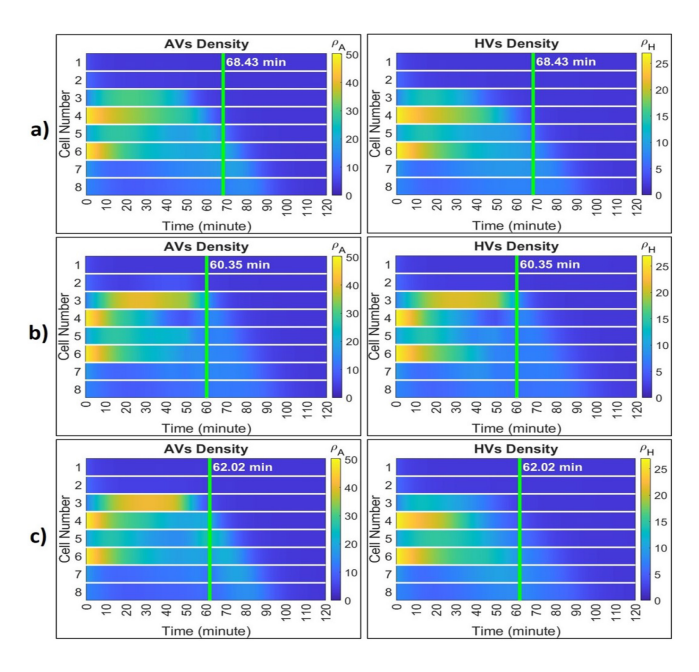


Fig. 4. Changes in the densities of highway cells over a 2-hour period for (a) No-Control, (b) Both-Class-Control, and (c) AVs-Class-Control scenarios.

 $\rho_{\text{Jam,A}}$  and  $\rho_{\text{Jam,H}}$  (the jam line) as shown in Fig. 3(b), while other cells remain in free-flow. The input flows to cell 1 are 355 veh/h/lane for AVs and 157 veh/h/lane for HVs.

Our traffic control objective is to alleviate congestion in cells [ $\mathcal{C}_4$   $\mathcal{C}_5$   $\mathcal{C}_6$ ], considered as the control block. To achieve this, the suggested velocity will be applied to cells 3, 4, 5, and 6, with the control input defined as  $u_c = [u_{3,c}, u_{4,c}, u_{5,c}, u_{6,c}]^T$ . The simulation time step is 5 seconds, with an MPC control period of 1 minute, a prediction horizon of  $N_p = 20$ , and a control horizon of  $N_u = 10$ . The MPC control period is set longer than the time step because frequent speed limit adjustments, such as every few seconds, are impractical in real-world scenarios. A longer control period aligns better with realistic speed management. The diagonal weight matrices used in the MPC optimization in (13) are  $\Omega = 0.1 \times I_m$ ,  $R = 30 \times I_m$ , and  $S = 100 \times I_m$ .

Fig. 4 shows the density changes of AVs and HVs in cells over a period of 2 hours. The green line indicates the point when all cells, not just those in the control block, reach the free-flow state. Without control, it takes about 68 minutes for congestion to clear. However, with FL-MPC applied to both AVs and HVs [Fig. 4(b)], congestion is resolved 11% faster, in approximately 60 minutes. When FL-MPC is applied only

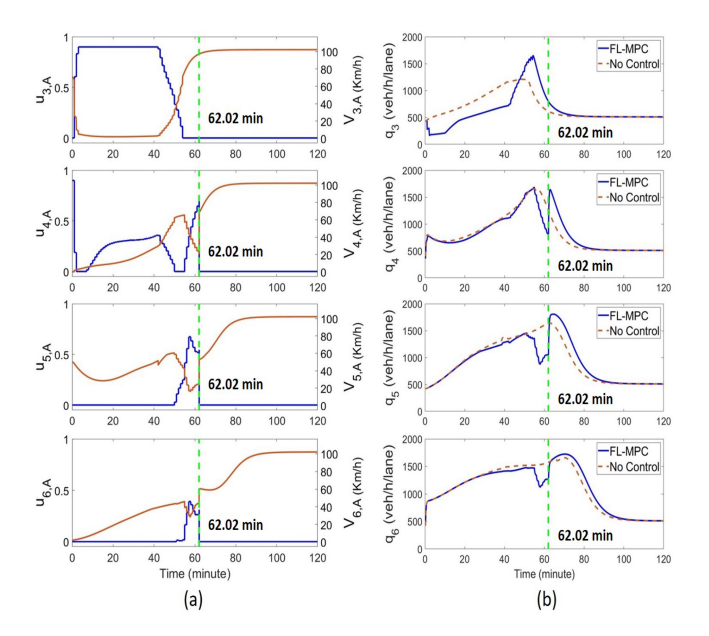


Fig. 5. Control block cells' (a) input (blue), suggested velocity (red), and (b) flow for AVs-Class-Control scenario.

to AVs [Fig. 4(c)], congestion clears 9% faster than without control, in around 62 minutes.

By examining the density variation across cells, it is clear that the FL-MPC leverages cell capacity before the control block by concentrating vehicles in those cells, enabling the control block to exit congestion more quickly. Specifically, Fig. 4(b) shows that cell C<sub>3</sub> briefly experiences congestion, which helps reduce congestion in downstream cells more quickly, ultimately leading to faster overall congestion relief. Additionally, controlling AVs alone [Fig. 4(c)] shows significant benefits. It achieves nearly the same reduction in congestion time as controlling both AVs and HVs, while requiring fewer interventions. This demonstrates the effectiveness of targeting AVs control, as it can significantly improve overall traffic flow with less control effort required.

Fig. 5 shows the control commands and traffic flow for the scenario where only AVs receive commands. Specifically, Fig. 5(a) shows the regulatory control command  $u_A$  and the suggested velocity  $U_A$ . For our simulations to prevent excessive deceleration and avoid commanding the vehicle to a full stop, we set  $u_{\text{max,c}} = 0.9$  ensuring safety. Fig. 5(a) shows that controller effectively keeps the control commands and suggested velocities within the limits. It is noteworthy that when  $u_{i,A} = u_{\text{max},A}$ , the controller recommends lower vehicle velocities (see (3)). To reduce congestion, the controller frequently suggests a low velocity for vehicles in Cell  $\mathcal{C}_3$ , which slows down the inflow to Cell  $\mathcal{C}_4$ , leading to the density concentration observed in Fig. 4. In contrast, Cell C<sub>6</sub> often receives a control value of zero, allowing vehicles to exit at the maximum possible velocity. It is noteworthy that this maximum velocity is not necessarily the free-flow speed but is also influenced by the cell's density (see (3) and (4)). Notably, there is always at least one zero control command at any time. This results from the constraint mapping algorithm, where a zero row in  $H_c^*$  enforces a zero control command

Fig. 5(b) shows the total traffic flow  $(q_{i,A} + q_{i,H})$  for the cells in the control block. The FL-MPC controller intentionally slows down the vehicles, explaining why the red line (no control) initially shows higher flow. However, after 62 minutes, as congestion is relieved, the controlled scenario (blue line) experiences more flow, as traffic becomes smoother. The flow finally merges to the inflow flow.

#### V. CONCLUSION

This letter presents a novel approach to managing heterogeneous traffic with both HVs and AVs using a FL-MPC framework. It addresses the challenges of nonlinear traffic dynamics and input constraints by integrating FL and MPC to ensure that control commands stay within bounds. A new constraint mapping algorithm ensures feasible solutions, even for over-actuated systems. Simulation results demonstrate the effectiveness of the approach in reducing congestion faster compared to uncontrolled systems. Future work will focus on addressing uncertainties in model parameters.

#### REFERENCES

- J. Li, C. Yu, Z. Shen, Z. Su, and W. Ma, "A survey on urban traffic control under mixed traffic environment with connected automated vehicles," *Transp. Res. Part C, Emerg. Technol.*, vol. 154, Sep. 2023, Art. no. 104258.
- [2] K. Chavoshi and A. Kouvelas, "Nonlinear model predictive control for coordinated traffic flow management in highway systems," in *Proc. Eur. Control Conf. (ECC)*, 2020, pp. 428–433.
- [3] K. Chavoshi, A. Ferrara, and A. Kouvelas, "A feedback linearization approach for coordinated traffic flow management in highway systems," *Control Eng. Pract.*, vol. 139, Oct. 2023, Art. no. 105615.
- [4] R. C. Carlson, I. Papamichail, and M. Papageorgiou, "Local feedback-based mainstream traffic flow control on motorways using variable speed limits," *IEEE Trans. Intell. Transp. Syst.*, vol. 12, no. 4, pp. 1261–1276, Dec. 2011.
- [5] M. J. Kurtz and M. A. Henson, "Input-output linearizing control of constrained nonlinear processes," *J. Process Control*, vol. 7, no. 1, pp. 3–17, 1997.
- [6] M. J. Kurtz, G.-Y. Zhu, and M. A. Henson, "Constrained output feedback control of a multivariable polymerization reactor," *IEEE Trans. Control* Syst. Technol., vol. 8, no. 1, pp. 87–97, Jan. 2000.
- [7] P. Karimi Shahri, B. HomChaudhuri, A. Ghaffari, and A. H. Ghasemi, "Improving the performance of a hierarchical traffic flow control framework using Lyapunov-based switched Newton extremum seeking," ASME Lett. Dyn. Syst. Control, vol. 3, no. 4, 2023, Art. no. 41003.
- [8] A. Rahmanidehkordi and A. Ghasemi, "Enhancing traffic flow via feed-back linearization and model predictive control under input constraints," presented at Modeling Estimation Control Conf., 2024.
- [9] S. Liu, B. De Schutter, and H. Hellendoorn, "Model predictive traffic control based on a new multi-class METANET model," *IFAC Proc. Vol.*, vol. 47, no. 3, pp. 8781–8786, 2014.
- [10] S. Logghe and L. H. Immers, "Multi-class kinematic wave theory of traffic flow," *Transp. Res. Part B, Methodol.*, vol. 42, no. 6, pp. 523–541, 2008.
- [11] S. Logghe, "Dynamic modeling of heterogeneous vehicular traffic," Ph.D. dissertation, Faculty Appl. Sci., Katholieke Universiteit Leuven, Leuven, Belgium, 2003.
- [12] J.-J. E. Slotine and W. Li, Applied Nonlinear Control. Englewood Cliffs, NJ, USA: Prentice Hall, 1991.
- [13] A. Hegyi, B. De Schutter, and J. Hellendoorn, "Optimal traffic control in freeway networks with bottlenecks," *IFAC Proc. Vol.*, vol. 38, no. 1, pp. 96–101, 2005.